

## Coastal impacts of offshore meso-scale eddies through the Kuroshio variation

Kaoru ICHIKAWA\* and Atsushi KANEDA\*\*

**Abstract :** In order to assess the influence of offshore meso-scale eddies in coastal areas facing to the Kuroshio, temperature data in the Bungo Channel and altimetry sea surface height (SSH) data are analyzed. It is east of Okinawa, far away from the Bungo Channel, where the SSH variation is most strongly correlated with the coastal temperature changes with periods of several weeks to months. Complex empirical orthogonal function analysis of the SSH variation indicated strong coherency with the coastal temperature for a train of meso-scale eddies propagating northeastward from east of Okinawa to south of Shikoku, suggesting that variations of the Kuroshio in front of the Bungo Channel induce the coastal temperature changes. However, in areas other than east of Okinawa and south of Shikoku, larger SSH variations which would not correlate well with the coastal temperature variations are detected showing that cross correlation with the coastal temperature is not significant in these regions.

**Key words :** meso-scale eddies, Bungo Channel, Kuroshio, Complex EOF analysis

### 1. Introduction

Although oceanic conditions in coastal areas are subject to many factors, influences of offshore variations are known to be one of the major factors in southern Japanese coasts facing to the Kuroshio. Using abundant coastal observations, many past researches have examined coastal variations in connection with the Kuroshio (e. g., KANEDA *et al.*, 1996; MATSUYAMA *et al.*, 1999).

Recently, longer time series of satellite altimetry data are available, which provide good description of sea surface dynamic height variations in offshore regions. In the present paper, we used those good descriptive data, both coastal and offshore, and related coastal temperature variations in the Bungo Channel (Fig. 1) to the offshore dynamic height variations by calculating their cross correlation. Furthermore, using complex empirical orthogonal function (CEOF) analysis of the

altimetry data, distinct movement pattern of meso-scale eddies coherent with the coastal temperature variations are extracted, and influence of the offshore meso-scale eddies on the coastal temperature is discussed.

The present paper consists of 6 sections: Data sets of temperature in the Bungo Channel and altimetry sea surface height are described in the next Section 2. Then results of their cross correlations are shown in Section 3. In Section 4, simple introduction of CEOF analysis is first presented, followed by corresponding results for the altimetry data, which are then used to interpret movement patterns of meso-scale eddies affecting to the coastal temperature changes. Discussion and conclusions of the results are summarized in Sections 5 and 6, respectively.

### 2. Data

#### 2.1. Coastal temperature data

Mooring stations have been deployed mainly by Ehime Prefectural Fisheries Laboratory and Ehime University to monitor water temperature along the eastern side of the Bungo Channel (Fig. 1). In the present analysis, 5m-depth water temperature record at the station K5 in

\* Research Institute for Applied Mechanics, Kyushu University, Fukuoka, Japan also, Frontier Observational Research System for Global Change, Tokyo, Japan

\*\* Center for Marine Environmental Studies, Ehime University, Matuyama, Japan

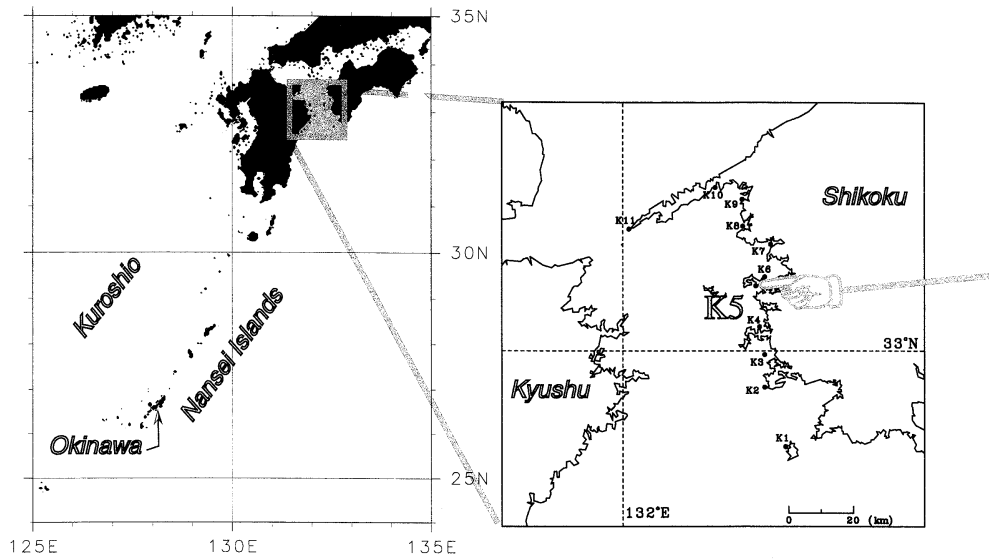


Fig. 1. Location of the Bungo Channel and mooring stations.

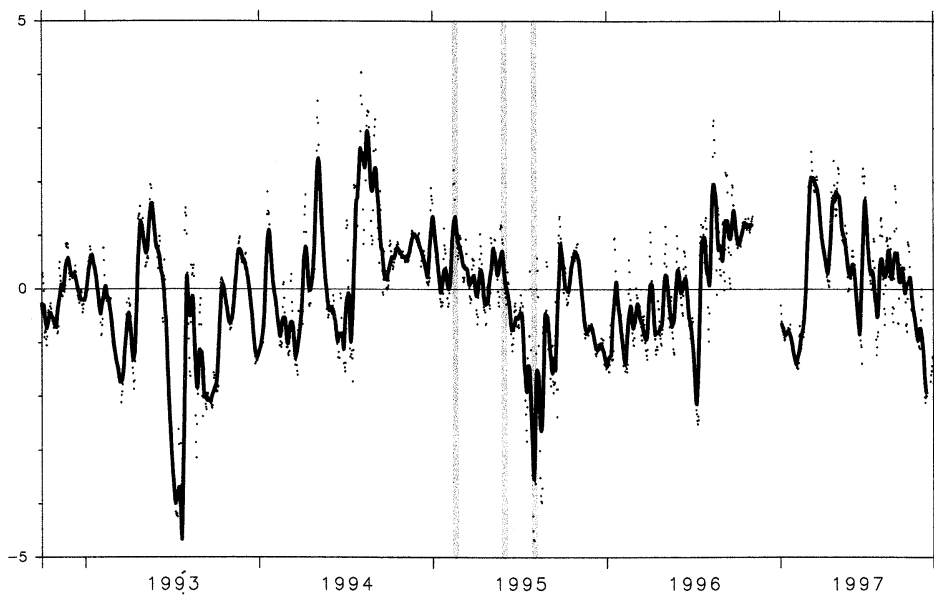


Fig. 2. Time series of daily temperature anomalies (dots) and their 10-day running means (line) at the station K5. Vertical lines indicate the dates corresponding to Fig. 6.

Shitaba Bay is used from October 1992 to November 1997 when the altimetry data are available.

The coastal temperature is obviously dominated by an annual cycle mainly determined by heat flux variations. In order to focus on

temperature changes induced by meso-scale eddies, we should extract this annual variation. Sinusoidal temperature variation with an annual cycle is estimated by the harmonic analysis of 5 years of 30-minute temperature data and extracted to obtain temperature anomaly;

Figure 2 shows time series of daily-averaged temperature anomalies. In addition, for further comparizon with altimeter data, daily temperature anomaly data is averaged over same 10 day periods with altimetry data.

## 2.2. Altimetry data

For altimetry data, we use all TOPEX/POSEIDON, ERS-1 (phase C, E, F and G) and ERS-2 data which are provided by AVISO as CORSSH. The CORSSH products are supplied by the CLS Space Oceanography Division, Toulouse, France (AVISO, 1996; LE TRAON *et al.*, 1995; LE TRAON and OGOR, 1998).

From those data, sea surface height (SSH) deviation from the climatological mean (Y1, 1995) is estimated at  $0.5^\circ$  grid pints in a study area south of Japan ( $125^\circ$ – $135^\circ$ E,  $24^\circ$ – $35^\circ$ N; left panel of Fig. 1) for each 10-day period from October 1992 for 5 years by an optimal interpolation similar to ICHIKAWA and IMAWAKI (1996) with spatial and temporal scales to be larger than approximately 150 km and 17 day, respectively (see YASUDA *et al.* (2000) and ICHIKAWA (2000) for more description of the optimal interpolation method used). Areas are excluded in the present analysis when the estimated error exceeds 99% of the root-mean-squared magnitude of SSH variations, and they are generally on the coastal boundary where less altimetry data are available. For the consistency with the coastal temperature anomaly data, sinusoidal annual SSH variation estimated from 5-year data is removed for each grid point.

## 3. Correlation between coastal and offshore variations

Cross correlation between the coastal temperature anomaly and the offshore SSH anomaly is calculated fo 5 year (189 10-day cycles). Spatial distribution of the correlation coefficient is shown in Fig. 3. The stronger positive (or negative) correlation becomes, the more frequently temperature in the Bungo Channel changes warmer (or colder) when the SSH anomaly increases. In this figure, statistically insignificant correlation coefficients indicated by the Student-*t* test with 95% confidence level are masked.

Significant correlations are found to be

positive south of Shikoku and east of the Tokara strait ( $132^\circ$ E,  $29^\circ$ N), and negative east of Okinawa and Kyushu. Note that there exists no significant correlation in front of the Bungo Channel. Also the strongest correlation in the study area is located east of Okinawa island, more than 700 km away from the channel. These results would suggest that either the temperature anomaly in the Bungo Channel is remotely controlled by SSH variations east of Okinawa island, or there exists a coherent variation which affects both the temperature anomaly in the Bungo Channel and the SSH anomaly east of Okinawa, but it does not dominate the SSH variation in front of the channel.

In the next setion, we perform CEOF analysis on the SSH anomaly in order to separate a SSH pattern corresponding to the temperature anomaly variations in the Bungo Channel from the other SSH patterns. By studying the separated SSH pattern, we would be able to interpret the distribution characteristics of the cross

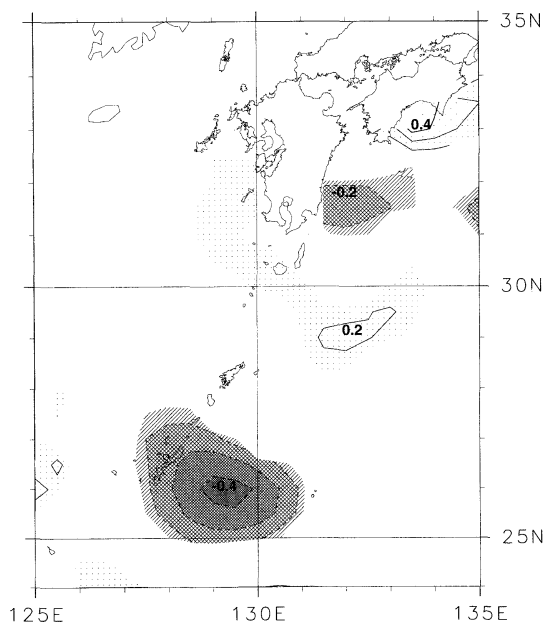


Fig. 3. Spatial distribution of cross correlation coefficient between the coastal temperature anomaly changes and the offshore SSH variations. Contour interval are 0.1 and positive (negative) correlations are shaded with dots (lines). Statistically insignificant values are masked in the figure.

correlation as shown in Fig. 3.

**4. Decomposition by CEOF modes**

**4.1. CEOF analysis of offshore SSH variations**

In CEOF analysis, SSH anomaly  $z(x, t)$  at a given position  $x$  and time  $t$  is decomposed into orthogonal complex modes  $C_j(x, t)$  as

$$z(x, t) \simeq \sum_j^N Re\{C_j(x, t)\}, \tag{1}$$

$$C_j(x, t) = A_j(x) e^{i\phi_j(x)} B_j(t) e^{i\varphi_j(t)}, \tag{2}$$

where  $N$  is the number of significant modes,  $A_j(x)$  spatial amplitude factor,  $\phi_j(x)$  spatial phase distribution,  $B_j(t)$  temporal mode amplitude, and  $\varphi_j(t)$  temporal phase variation (e. g. BARNET, 1983; WHITE *et al.*, 1987).

The value so-called contribution ratio,  $R_j$ , is often used to account for the contribution of a given mode  $j$  to explain overall variance of  $z(x, t)$ , and is defined by

$$R_j = \frac{\int \int |C_j(x, t)|^2 dx dt}{\int \int z^2(x, t) dx dt} \tag{3}$$

By adopting a normalization condition  $\int A_j^2(x) dx = 1$  for any mode  $j$ , and by assuming that the sum of  $N$  CEOF modes in Equation (1) well represent the overall variance of  $z(x, t)$ , the above Equation (3) can be simplified as

$$R_j = \frac{\int B_j^2(t) dt}{\sum_k^N \int B_k^2(t) dt} \tag{4}$$

In addition, we can define "local contribution ratio",  $R_j^l(x_0)$ , for a given mode  $j$  at a given location  $x_0$  as

$$R_j^l(x_0) = \frac{\int |C_j(x_0, t)|^2 dt}{\int z^2(x_0, t) dt}$$



Fig. 4. Contribution ratio  $R_j$  of each CEOF mode to the SSH variance.

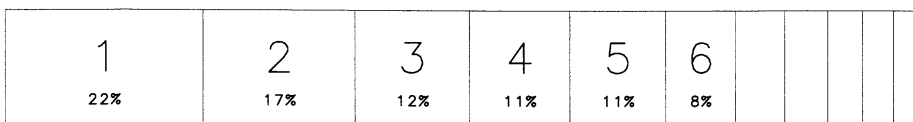


Fig. 5. Contribution ratio of each CEOF mode to decompose temporal variations of the temperature

$$= \frac{A_j^2(x_0) R_j}{\sum_k^N A_k^2(x_0) R_k} \tag{5}$$

The CEOF analysis is performed on the 5-year SSH anomaly in the study area. We select first 11 modes as significant CEOF modes ( $N = 11$ ) such that their contribution ratio  $R_j$  exceed 2% and the sum of these modes explains more than 80% of total SSH variance. Contribution ratio  $R_j$  of each mode is shown in Fig. 4. One may notice that there is no significant domination by a single mode. This is mainly because significant annual signals are removed before CEOF analysis, and also because movements of meso-scale eddies in this area are complicated due to interactions with the Kuroshio current.

**4.2. Decomposition of coastal temperature data**

Using temporal amplitude and phase variations of CEOF modes,  $B_j(t)$  and  $\varphi_j(t)$ , time series of the coastal temperature anomaly,  $T(t)$ , can be decomposed by harmonic analysis. In other words, we would determine unknown amplitude factor  $F_j$  and phase constant  $\theta_j$  in an estimate  $\tilde{T}(t)$  by minimizing  $\int (T(t) - \tilde{T}(t))^2 dt$ , where

$$\tilde{T}(t) = \sum_j^N Re\{F_j B_j(t) e^{i(\varphi_j(t) + \theta_j)}\} \tag{6}$$

By replacing  $A_j(x)$  and  $\phi_j(x)$  in Equation (2) by  $F_j$  and  $\theta_j$ , contribution ratio of each CEOF mode for explaining the variance of the coastal temperature anomaly can be defined as

$$R_j^T = \frac{F_j^2 R_j}{\sum_k^N F_k^2 R_k}, \quad (7)$$

similarly to the local contribution in Equation (5).

Figure 5 shows values of  $R_j^T$  for all 11 modes. Clearly in the figure, contribution of the 8th mode  $R_8^T$  becomes significantly large, despite the fact that the SSH variation of that mode explains only 4% of the overall SSH variations (Fig. 4). This increase of contribution ratio of the 8th mode suggests that the coastal temperature is highly sensitive to the SSH variation pattern of that mode.

Examples of the SSH variation for the CEOF 8th mode,  $Re\{C_8(x,t)\}$ , in 1995 are shown in Fig. 6; vertical lines in Fig. 2 show corresponding dates. The temporal phase variation of this mode  $\varphi_8(t)$  around these dates is plotted in Fig. 7. In this figure, unreliable phase estimates based on smaller mode amplitude  $B_8(t)$  are marked by asterisks when area variance  $\int |C_8(x,t)|^2 dx = B_8(t)^2$  becomes less than  $1 \text{ cm}^2$ . From east of Nansei islands to south of Shikoku, a train of cyclonic and anti-cyclonic eddies with the size of approximately 200–400 km is seen in Fig. 6, as indicated by “A”–“F”. These meso-scale eddies seem to propagate northeastward, or in the downstream direction of the Kuroshio, at a speed of approximately 4 cm/s during this period (Figs. 6 and 7).

Comparing with the coastal temperature anomaly in the Bungo Channel in Fig. 2, cyclonic and anti-cyclonic meso-scale eddies agree well with the distribution pattern of the cross correlation coefficient between the SSH anomaly and the coastal temperature anomaly shown in Fig. 3. In Fig. 6c when the coastal temperature shows sharp decrease (Fig. 2), eddies with positive SSH anomaly are present in the east of Okinawa (F) and east of Kyushu (B), and those with negative SSH anomaly are found in the south of Shikoku (A) and east of the Tokara strait south of Kyusyu (C). Meanwhile, the sign of SSH anomaly becomes opposite in Fig. 6a when the coastal temperature anomaly is largely positive. The location of the eddies seems subtle since amplitude of the coastal temperature anomaly is not large when the position of these eddies is slightly shifted in Fig. 6b.

The existence of meso-scale eddies can be noticed in Fig. 6 in front of the Bungo Channel, which is not clear in the cross correlation analysis in Fig. 3. These eddies correspond to variations of the Kuroshio, and it seems to be physically more realistic to interpret that the coastal temperature variation is directly caused by variations of the Kuroshio, rather than being remotely controlled by meso-scale eddies east of Okinawa. Since the coastal temperature is largely affected by slight move-

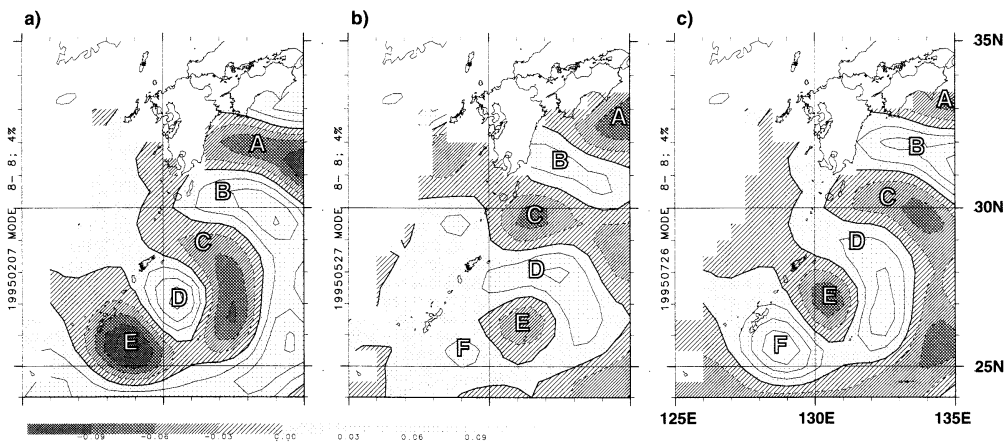


Fig. 6. The SSH anomaly of CEOF 8th mode on 7 February (a), 27 May (b) and 26 July, 1995 (c). Contour intervals are 3 cm and negative values are heavily shaded. Characters “A” to “F” are shown for convenience of discussions.

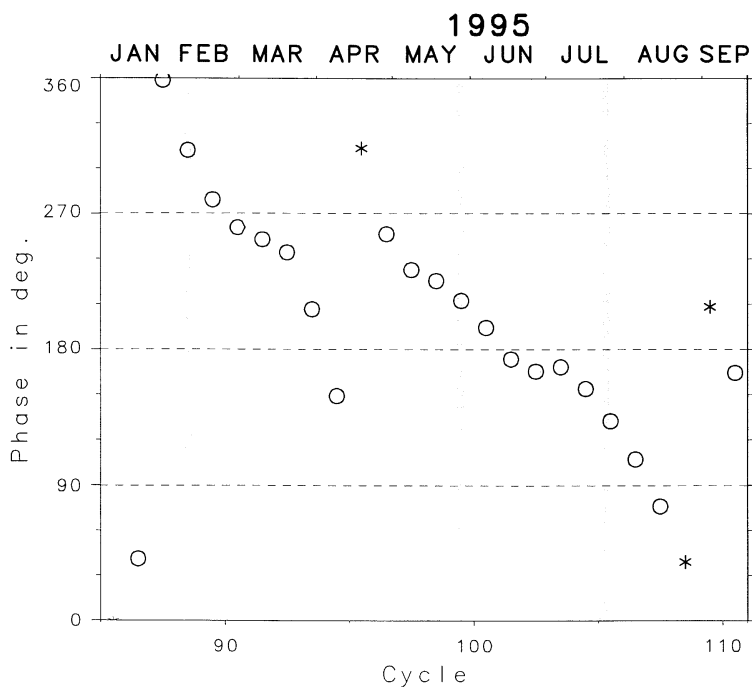


Fig. 7. Temporal phase variation of the CEOF 8th mode,  $\varphi_8(t)$  in 1995. In this figure, asterisks indicate unreliable estimation. Vertical lines indicate the dates shown in Fig. 6. Numbers at the bottom indicate the altimetry 10-day cycles.

ment of the eddies as seen in Fig. 6, the idea, that the coastal temperature variation is directly caused by the eddies closer to the Bungo Channel, would be also circumstantially supported.

The reason why the meso-scale eddies in front of the Bungo Channel are not clearly seen in the cross correlation coefficient (Fig. 3) would be explained by referring to a map of local contribution ratio for the CEOF 8th mode  $R_8^T$  shown in Figure 8. The local Contribution ratio of the 8th mode  $R_8^T$  has largest value in areas east of Okinawa and south of Shikoku, meanwhile  $R_8^T$  is less than 5% in front of the Bungo Channel. In the areas with small  $R_8^T$  such as in front of the Bungo Channel, SSH variations of the other CEOF modes than the 8th would be present whose amplitudes surpass that of the 8th mode and which may not correlate with the coastal temperature variations. In such a case, cross correlation coefficient between the SSH and the coastal temperature would be statistically insignificant even

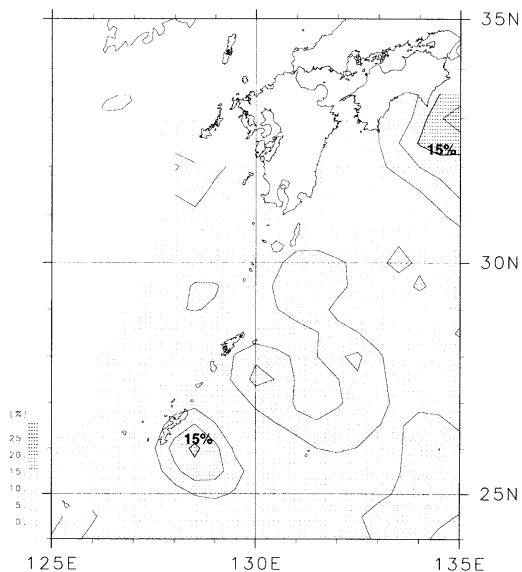


Fig. 8. Map of the local contribution ratio for the CEOF 8th mode,  $(\chi)$ . Areas with larger ratio are heavily shaded. Contour intervals are 5%.

though there may exist moderate SSH variations given by the CEOF 8th mode which correlate well with the coastal temperature changes. On the contrary, in the areas with larger  $R_s^2$ , the SSH variation would be more similar to that of the 8th mode alone seen in Fig. 6, so that the cross correlation coefficient would become statistically significant.

## 5. Discussions

Although the coastal temperature anomaly in the Bungo Channel is found sensitive to the SSH anomaly of the CEOF 8th mode, physical reasons are not considered in the present paper. The anti-cyclonic meso-scale eddy "B" in front of the channel in Fig. 6c, which is elongated in the direction normal to the Kuroshio axis, indicates that the Kuroshio axis is located slightly closer to the channel when the coastal temperature becomes cold. This relationship between the closer Kuroshio path and colder coastal temperature is consistent with hydrographic observations in the Bungo Channel in 1993, which indicate intrusion of offshore cold bottom water when the Kuroshio took a slightly closer path (KANEDA *et al.*, 1996). This intrusion may be induced by shoreward bottom Ekman transport enhanced by the near-shore Kuroshio path flowing over the shelf. Another interpolation, however, can be obtained from Fig. 6c that seaward surface velocity in the Bungo Channel is accelerated when the coastal temperature decreases, which may also result in intrusion of cold bottom water by assuming simple mass conservation at the mouth of the channel. More in situ observational results are necessary to understand physical processes of water exchange in the channel.

Also in the present paper, physical interpretation of the CEOF 8th mode itself has not been discussed. One may notice that the eddies east of Nansei islands propagate northeastward, similarly in the Kuroshio region east of Kyushu and south of Shikoku where northeastward advection is strong. This may suggest the existence of strong northeastward current east of Nansei islands, although extensive observations are again necessary to study this possibility.

One may remind outstanding *kyucho* events

in the Bungo Channel as an example of strong influences of the Kuroshio in the channel (e. g. TAKEOKA *et al.*, 1993). Unfortunately, *kyucho* is out of scope in the present analysis since spatial and temporal resolutions of the altimetry data are too coarse to detect *kyucho* events. We may define, however, frequency of *kyucho* occurrences during a certain period to cope with low resolutions of the SSH data, although we shall leave this for study in the future.

We used the temperature data at the station K5 only to represent variations of the whole Bungo Channel. This could be a severe problem for small-scale phenomena such as *kyucho* events, but it should be acceptable in the present analysis since our interest is limited to variations of larger scales. Rather, use of the data at the eastern side of the channel may induce some quantitative discrepancy from the area average, although apparent qualitative characteristics in Fig. 2 would not be altered (KANEDA *et al.*, 1996).

## 6. Conclusions

Temperature variations in the Bungo Channel are interpreted with respect to the offshore sea surface height (SSH) variations obtained from altimetry data. In order to focus on variations induced by meso-scale eddies, sinusoidal variations with an annual cycle are first removed from both the SSH and the coastal temperature data.

Cross correlation between these two data sets indicates that the SSH variation east of Okinawa, more than 700 km away from the Bungo Channel, shows the strongest correlation in the study area. On the contrary, correlation coefficient in front of the Bungo Channel is statistically insignificant.

Complex empirical orthogonal function (CEOF) analysis of the SSH anomaly is then performed to extract phase-propagating SSH patterns coherent with the coastal temperature variations. More than 30% of the variance of the coastal temperature changes are explained by the minor CEOF 8th mode, which is characterized by a train of meso-scale eddies propagating northeastward from east of Okinawa to south of Shikoku. Movements of these eddies in the CEOF 8th mode coincident well the

coastal temperature variation. This result would suggest that the temperature in the Bungo Channel is affected by the eddies close to the channel which corresponds to variations of the Kuroshio, rather than being remotely controlled by the far eddies. Distribution of the local contribution ratio of the CEOF 8th mode, however, indicates existence of SSH variations of the other CEOF modes in front of the channel whose amplitude is much larger than of the 8th mode and which may not correlate well with the coastal temperature variation, resulting in smaller cross correlation coefficient with the temperature in the Bungo Channel. Meanwhile, in the areas east of Okinawa and south of Shikoku, the SSH variation is more similar to that of the 8th mode alone, so that the cross correlation in these areas would remain evident.

Physical reasons of coherency between the coastal temperature variations and slight meanders of the Kuroshio in front of the Bungo Channel indicated by meso-scale eddies in the CEOF 8th mode are discussed. Also, possibility of a strong northeastward current east of Nansei islands is considered, referring to the northeastward propagation of the eddies both in the Kuroshio region and in the area east of Nansei islands.

#### Acknowledgments

We would like to thank Prof. H. TAKEOKA of Ehime University and Dr. Y. KOIZUMI of Ehime Prefectural Fisheries Experimental Station who kindly provided valuable temperature data set in the Bungo Channel. Mr. T. SAITO of National Research Institute of Fisheries Science contributed to discussions on interpretation of the results. Also, discussion with Dr. Y. MASUMOTO of the University of Tokyo were helpful. This research was supported in part by a Grant-in-Aid for Scientific Research from the Ministry of Education, Science, and Culture of Japan, and also by Core Research for Evolutional Science and Technology (CREST) of Japan Science and Technology Corporation (JST).

#### References

- AVISO (1996): AVISO Handbook for Merged TOPEX/POSEIDON Products. AVI-NT-01-101-CN, Edition 3.0.
- BARNET, T.P. (1983): Interaction of the monsoon and Pacific trade wind system at interannual time scales. Part I: The equatorial zone. *Mon. Wea. Rev.*, **111**, 756-773.
- ICHIKAWA, K. (2000): Variation of the Kuroshio in the Tokara Strait induced by meso-scale eddies. submitted to *J. Oceanogr.*
- ICHIKAWA, K. and S. IMAWAKI (1996): Estimating the sea surface dynamic topography from Geosat altimetry data. *J. Oceanogr.*, **52**, 43-68.
- KANEDA, A., H. TAKEOKA and Y. KOIZUMI (1996): Decrease of water temperature in the Bungo Channel in summer 1993. *Bull. Coastal Oceanogr.*, **34**, 71-78. (in Japanese with English abstract)
- LE TRAON, P. Y., P. GASPAR, F. BOYUSSEL and H. MAKHMARA (1995): Using TOPEX/POSEIDON data to enhance ERS-1 orbit. *J. Atm. Ocean. Tech.*, **12**, 161-170.
- LE TRAON, P. Y. and F. OGOR (1998): ERS-1/2 orbit improvement using TOPEX/POSEIDON: the 2cm challenge. *J. Geophys. Res.*, **103**(C4) 8045-8057.
- MATSUYAMA, M., H. ISHIDOYA, S. IWATA, Y. KITADE and H. NAGAMATSU (1999): Kyucho induced by intrusion of Kuroshio water in Sagami Bay, Japan. *Continental Shelf Res.*, **19**, 1561-1575.
- TAKEOKA, H., H. AKIYAMA and T. KIKUCHI (1993): The Kyucho in the Bungo Channel, Japan-Periodic Intrusion of Oceanic Warm Water (1987): *J. Oceanogr.*, **49**, 369-382.
- WHITE, W. B., S. E. PAZAN and M. INOUE (1987): Hindcast/Forecast of ENSO events based upon the redistribution of observed and model heat content in the western tropical Pacific, 1964-86. *J. Phys. Oceanogr.*, **17**, 264-280.
- YASUDA, I., S. ITOH, Y. SHIMIZU, K. ICHIKAWA, K. UEDA, T. HONMA, M. UCHIYAMA, K. WATANABE, N. SUNO, K. TANAKA and K. KOIZUMI (2000): Cold-core anti cyclonic eddies south of Bussol' Strait in the north-western Subarctic Pacific. *J. Physical Oceanogr.*, **30**, 1137-1157.
- YI, Y. (1995): Determination of Gridded Mean Sea Surface from TOPEX, ERS-1 and GEOSAT Altimeter Data, Rep. 434, Dept. Geod. Sci. Surv., The Ohio State Univ., Columbus.

*Received on January 27, 2000*

*Accepted on August 2, 2000*